

## Energetics of Self-Assembly and Chain Confinement in Silver Alkanethiolates: Enthalpy–Entropy Interplay

Andrey A. Levchenko,<sup>†</sup> Chanel K. Yee,<sup>‡</sup> Atul N. Parikh,<sup>‡</sup> and Alexandra Navrotsky<sup>\*,†</sup>

Thermochemistry Facility and NEAT ORU and Applied Science Department, University of California at Davis, Davis, California 95616

Received May 7, 2005. Revised Manuscript Received July 27, 2005

The formation enthalpies by in situ direct synthesis calorimetry for a series of silver alkanethiolates,  $\text{AgS}(\text{CH}_2)_n\text{CH}_3$ , with various long chain-length substituents ( $n = 9, 11, 15, \text{ and } 17$ ) are reported. The calorimetric results support a mechanism of stepwise hierarchical assembly involving primary directional interactions between Ag and S forming the inorganic core and secondary stacking facilitating the formation of the three-dimensional structure. The formation enthalpy data are chain-length dependent, indicating an energy of  $-4 \pm 0.5$  kJ/mol per methyl group due to alkyl chain interactions. The chain independent component of the enthalpy associated with bonding between Ag and S is  $-137 \pm 6$  kJ/mol, which is consistent with previous experimental data and ab initio calculations for these and related materials. A new recrystallization method offers significantly improved structural consistency across the chain-length series. Larger purified crystals, prepared by this method, were used to probe the structure, thermodynamics of phase transitions, and thermal stability, using a combination of differential scanning and solution calorimetry, thermogravimetric analysis, evolved gas Fourier transform infrared spectroscopy, and temperature-dependent X-ray diffraction. The DSC data show that the temperature of the main phase transition at 131 °C is essentially independent of the length of the alkyl chain substituents for recrystallized samples. This chain-length independence does not reflect constant enthalpy of transition but rather a complex interplay between enthalpic and entropic contributions. In agreement with previous studies, this phase transition is assigned to a fully reversible transformation from the layered crystalline structure to a columnar mesophase, characterized by structural rearrangements of the inorganic framework and partial conformational disordering of the chain substituents. In situ scanning calorimetry in toluene upon slow heating from room temperature to 110 °C, where the sample appeared to dissolve in the toluene near 100 °C, gives insight into chain assembly and crystal growth. The second reaction seen in DSC at 210 °C is an irreversible transformation to an amorphous derivative, ultimately leading to the formation of silver and silver sulfide crystals resulting from the chemical decomposition of alkyl chains.

### Introduction

In the last 15 years, there has been much activity in the area of self-assembly of alkanethiolates, including monolayers on transition metal surfaces (Au, Ag, Cu),<sup>1–8</sup> alkanethiolate covered metal nanoparticles,<sup>9,10</sup> and crystalline metal alkanethiolates.<sup>11–16</sup> Interest in the self-assembled

alkanethiolates pertains to their potential applications in industry for surface protection, lubrication, microelectronics, biosensing, and lithography.<sup>1</sup> The alkanethiolate monolayers on gold and silver surfaces are the most exploited and frequently studied systems. A great variety of experimental and theoretical methods has been successfully employed to achieve detailed description of the structure and properties of alkanethiolate monolayers. However, less is known about the energetics of self-assembly, particularly of silver alkanethiolates.<sup>17</sup> Thermodynamic studies include ab initio calculations of binding energies of alkanethiolate on gold and silver by Sellers et al.<sup>18</sup> and electrochemical measure-

\* Corresponding author. E-mail: anavrotsky@ucdavis.edu.

<sup>†</sup> Thermochemistry Facility and NEAT ORU.

<sup>‡</sup> Applied Science Department.

- (1) Ulman, A. *Chem. Rev.* **1996**, *96* (4), 1533.
- (2) Laibinis, P. E.; Whitesides, G. M.; Allara, D. L.; Tao, Y. T.; Parikh, A. N.; Nuzzo, R. G. *J. Am. Chem. Soc.* **1991**, *113* (19), 7152.
- (3) Walczak, M. M.; Chung, C. K.; Stole, S. M.; Widrig, C. A.; Porter, M. D. *J. Am. Chem. Soc.* **1991**, *113* (7), 2370.
- (4) Bryant, M. A.; Pemberton, J. E. *J. Am. Chem. Soc.* **1991**, *113* (22), 8284.
- (5) Fenter, P.; Eisenberger, P.; Li, J.; Camillone, N.; Bernasek, S.; Scoles, G.; Ramanarayanan, T. A.; Liang, K. S. *Langmuir* **1991**, *7* (10), 2013.
- (6) Dhirani, A.; Hines, M. A.; Fisher, A. J.; Ismail, O.; Guyotsonnest, P. *Langmuir* **1995**, *11*, 1 (7), 2609.
- (7) Heinz, R.; Rabe, J. P. *Langmuir* **1995**, *11*, 1 (2), 506.
- (8) Lai, Y. H.; Yeh, C. T.; Cheng, S. H.; Liao, P.; Hung, W. H. *J. Phys. Chem. B* **2002**, *106* (21), 5438.
- (9) Pradeep, T.; Sandhyarani, N. *Pure Appl. Chem.* **2002**, *74* (9), 1593.
- (10) Pradeep, T.; Mitra, S.; Nair, A. S.; Mukhopadhyay, R. *J. Phys. Chem. B* **2004**, *108* (22), 7012.
- (11) Dance, I. G.; Fisher, K. J.; Banda, R. M. H.; Scudder, M. L. *Inorg. Chem.* **1991**, *30* (2), 183.

- (12) Baena, M. J.; Espinet, P.; Lequerica, M. C.; Levelut, A. M. *J. Am. Chem. Soc.* **1992**, *114* (11), 4182.
- (13) Parikh, A. N.; Gillmor, S. D.; Beers, J. D.; Beardmore, K. M.; Cutts, R. W.; Swanson, B. I. *J. Phys. Chem. B* **1999**, *103* (15), 2850.
- (14) Bardeau, J. F.; Parikh, A. N.; Beers, J. D.; Swanson, B. I. *J. Phys. Chem. B* **2000**, *104* (3), 627.
- (15) Fijolek, H. G.; Grohal, J. R.; Sample, J. L.; Natan, M. J. *Inorg. Chem.* **1997**, *36* (4), 622.
- (16) Fijolek, H. G.; GonzalezDuarte, P.; Park, S. H.; Suib, S. L.; Natan, M. J. *Inorg. Chem.* **1997**, *36* (23), 5299.
- (17) Lavrich, D. J.; Wetterer, S. M.; Bernasek, S. L.; Scoles, G. *J. Phys. Chem. B* **1998**, *102*, 3456.
- (18) Sellers, H.; Ulman, A.; Shnidman, Y.; Eilers, J. E. *J. Am. Chem. Soc.* **1993**, *115* (21), 9389.

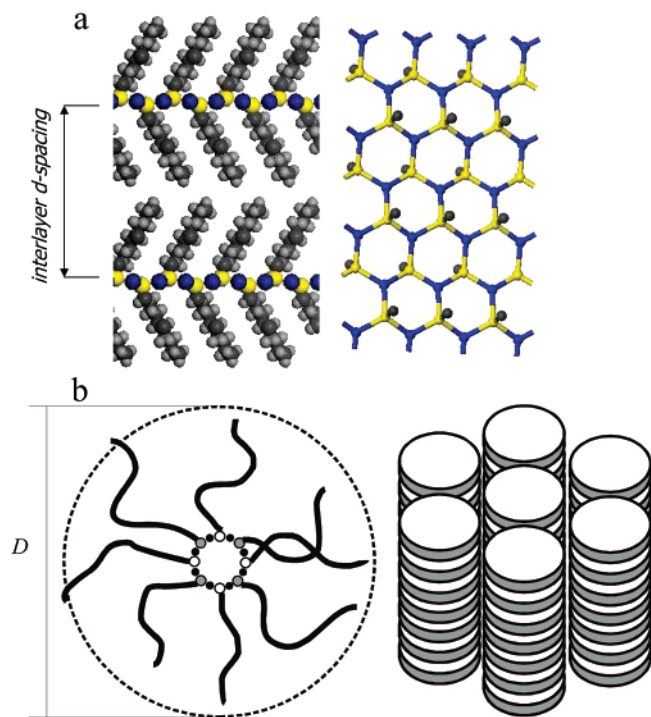


**Figure 1.** (a) Schematic representation of the layered structure of long-chain silver alkanethiolates at room temperature. The right panel indicates the trigonal coordination of Ag with S atoms resulting in a quasi-hexagonal inorganic core. (b) Schematic representation of the structure of the columnar (micellar) mesophase in long-chain silver alkanethiolates.

ments by Hatchett et al.<sup>19,20</sup> and Azzaroni et al.,<sup>21</sup> in which the free energies of oxidative adsorption of alkanethiolates on Ag in water and methanolic solutions, as well as their mixtures, were deduced from potentials of reductive electrodesorption.

In contrast to alkanethiolate monolayers, experimental techniques (e.g., calorimetry), suitable mainly for bulk materials, can be used to study layered silver alkanethiolates. These compounds can be synthesized simply by the slow addition of silver nitrate to a thiol solution  $\text{HS}(\text{CH}_2)_n\text{CH}_3$ . Previous studies have established that they adopt a common structural motif for a relatively wide range of chain lengths of the alkane substituents.<sup>11–14</sup> These crystals exhibit a periodically layered arrangement of bimolecular assemblies of organic thiols and the Ag–S inorganic core (Figure 1a). The Ag–S core is organized as a pseudo-two-dimensional puckered sheet with alternating Ag and S atoms, and the chain substituents extend on each side. The chains are packed in an ordered assembly sandwiched between the inorganic Ag–S backbones, comprising all-trans-extended chains. This structure is formed through stepwise hierarchical assembly involving primary directional interactions between Ag and S forming the inorganic core and secondary stacking facilitating the formation of the three-dimensional structure (Figure 1a).<sup>13,14</sup> Silver alkanethiolates resemble self-assembled monolayers in terms of the chain ordering and confinement at the organic–inorganic interface.

The prevalence of interfaces, dimensional confinement of chain assemblies, and covalent pinning of individual chains to the Ag–S inorganic framework all must influence the chain dynamics and phase behavior of silver alkanethiolates in nontrivial manners.<sup>22,23</sup> Indeed, a previous study by Baena et al.<sup>12</sup> proposed a complex phase diagram for silver alkanethiolates, reminiscent of liquid–crystalline mesophases. More recently, we examined the chain conformational dynamics during the temperature-induced phase transitions in silver *n*-dodecanethiolate using temperature-programmed Fourier transform infrared spectroscopy.<sup>14</sup> We found that the transition at 130 °C was fully reversible and attributed to rapid accumulation of gauche conformers via partial disordering of alkyl chains.

We believe that calorimetric studies of these systems should improve our knowledge about mechanisms of self-assembly, temperature-dependent phase behavior, chain dynamics, and stability of alkyl chains in confined geometries. Here, we are particularly interested in examining how the bonding and interactions at the pervasive organic–inorganic interfaces influence the thermodynamic driving forces, namely, enthalpy and entropy, in the formation and phase transitions of these complex solids. In this respect, results for monolayer protected metal clusters or nanoparticle architectures cannot be unambiguously applied to alkyl layers on a flat surface due to surface curvature and reported low coverage. Therefore, silver alkanethiolate crystals are more adaptable systems to study the energetics of the formation (self-assembly) by calorimetric techniques.

In this study, we used three types of calorimetric experiments to elucidate the energetics of self-assembly of silver alkanethiolate, as well as the phase transformations. In situ reaction calorimetry, in which the silver alkanethiolate was formed directly from alkanethiol and silver nitrate in acetonitrile at room temperature, measured formation enthalpies and, by systematically varying the alkyl chain length, distinguished contributions to the total enthalpy originating from van der Waals interactions between alkyl chains and Ag–S bond formation. Here, the formation enthalpies for silver alkanethiolates are obtained experimentally. Scanning calorimetry in a closed system is a Calvet microcalorimeter involving heating and cooling silver alkanethiolate samples in toluene, in which they dissolve on heating and recrystallize on cooling. These experiments provided insights into stacking assembly, probably without breaking Ag–S bonds, of preformed bilayers. Differential scanning calorimetry of recrystallized solvent-free samples provided temperatures, enthalpies, and entropies of the phase transitions.

Interestingly, we found that in accord with the DSC data reported by Baena et al.,<sup>12</sup> the temperature of the conformational transition at 131 °C is essentially (variations less than 1 °C) independent of the chain length. From the viewpoint of thermochemistry, this chain-length independent structural transition poses an important question: does the constant transition temperature imply constant enthalpy of

(19) Hatchett, D. W.; Stevenson, K. J.; Lacy, W. B.; Harris, J. M.; White, H. S. *J. Am. Chem. Soc.* **1997**, *119* (28), 6596.

(20) Hatchett, D. W.; Uibel, R. H.; Stevenson, K. J.; Harris, J. M.; White, H. S. *J. Am. Chem. Soc.* **1998**, *120* (5), 1062.

(21) Azzaroni, O.; Vela, M. E.; Andreasen, G.; Carro, P.; Salvarezza, R. *C. J. Phys. Chem. B* **2002**, *106* (47), 12267.

(22) Bhushan, B.; Israelachvili, J. N.; Landman, U. *Nature* **1995**, *374* (6523), 607.

(23) Granick, S. *Phys. Today* **1999**, *52* (7), 26.

transition or does it reflect a complex compensation of enthalpy and entropy factors? Addressing this question will provide significant new insight into the effects of confined geometry and the role of chain disordering in determining the thermal phase behavior of silver alkanethiolates and may illustrate the thermal properties of broader classes of organic–inorganic nanomaterials. While thermal analysis measurements for many silver alkanethiolates have been made previously,<sup>24,25</sup> this issue has not been fully addressed.

Previous studies aimed at determining thermodynamic phase behaviors of silver alkanethiolates have utilized as-synthesized materials. These exhibit considerable variations in the temperatures of transitions and transition enthalpies, which can be ascribed to variations in sample purity due to the differences in the synthetic details and thermal history of the samples. In this study, we employed a simple recrystallization strategy that yields structurally uniform silver alkanethiolate samples for a wide range of chain-length substituents. We also correct calorimetric results to the isothermal situation by varying the heating rate.

Thiolates with  $n = 9, 11, 15,$  and  $17$  were chosen in the study because they represent a structurally self-consistent series, characterized by the same number and sequences of phase transitions. Powder X-ray diffraction was used to confirm structure of the thiolates at room and elevated temperatures. We employed thermogravimetric analysis to fill the information gap in previous studies about thermal stability and decomposition of the materials. In another publication, we will also address in detail the crystal structure of silver alkanethiolates obtained by X-ray diffraction using synchrotron radiation and ab initio calculations.<sup>26</sup>

## Experimental Procedures

**Materials.** All  $n$ -alkanethiols ( $\text{CH}_3(\text{CH}_2)_n\text{SH}$ ,  $n = 9, 11, 15,$  and  $17$ ;  $>97\%$  purity) were received from Aldrich and used without further purification. Silver nitrate ( $\text{AgNO}_3$ ) was purchased from Bio-Analytical Systems, Inc. (West Lafayette, IN). Triethylamine ( $(\text{C}_2\text{H}_5)_3\text{N}$ , 99.5%) was obtained from Fluka Chemical Co. Acetonitrile and toluene were HPLC grade quality ( $>99.7\%$ ) from Aldrich and used as received.

**Sample Synthesis.** Detailed preparation procedures for silver alkanethiolates have been reported elsewhere.<sup>11,13,14</sup> Briefly, silver alkanethiolates under study were precipitated by dropwise addition (1 mL/min) of a silver nitrate solution (40 mM) in acetonitrile into a mixture of thiol (40 mM) and triethylamine (40 mM) also in acetonitrile. The mixture of thiol and triethylamine was sonicated for about 1 h. To minimize light exposure, the reaction vessels were wrapped in aluminum foil. After the  $\text{AgNO}_3$  solution was added, the mixture was stirred overnight. Then, the solution was isolated by suction filtration and thoroughly washed with acetonitrile. The resulting powders were almost white for all the thiolates. The silver alkanethiolates are reported to be highly insoluble in almost all solvents except for hot toluene near its boiling point. To enhance crystallinity, the samples were recrystallized in toluene maintained at  $110^\circ\text{C}$  and then cooled to room temperature under ambient

conditions. The samples were then washed with toluene and acetone at room temperature and dried for several hours (typically, overnight) in a vacuum oven. The recrystallized samples varied in color from bright yellow to opaque brown. According to earlier studies of structurally analogous silver thiolates, AgSRs with triply coordinated Ag are yellow, whereas purely double coordinated compounds are white. This concept contradicts recent studies of short-chain silver thiolates by Fijolek et al.<sup>15,16</sup> They believe that the yellow color is related to the presence of gauche conformers in silver thiolates. Taking into account the recent work of Bansebaa et al.,<sup>24</sup> where diagonal coordination of Ag in long-chain silver thiolates is supported by UV–vis spectroscopy, it is unclear how color is related to the structure of the material. In agreement with their work, we found no indication of any significant population of the gauche form for long-chain silver thiolates.<sup>13,14</sup> We will not address this issue further because it lies beyond the scope of this publication.

**Powder X-ray Diffraction.** Powder X-ray diffraction (XRD) was performed on a Scintag Pad-V diffractometer operated in reflection mode at 45 kV and 40 mA using Cu  $K\alpha$  radiation ( $\lambda = 1.54056 \text{ \AA}$ ). The diffractometer was calibrated with quartz as a standard. Sample powders were mounted in a zero-background quartz holder, and data were collected from  $2$  to  $100^\circ 2\theta$  in a step scan mode with an angular resolution of  $0.02^\circ$ .

XRD patterns at elevated temperatures were collected in an inert helium environment on an Inel-CPS120 diffractometer equipped with a linear position sensitive detector with a fixed angle of incidence. The samples were placed on a flat plate in a high-temperature furnace equipped with a temperature controller.

**Calorimetry.** Thermal analyses (TG/DSC) were performed in an argon atmosphere on a Netzsch STA 449 C apparatus. Temperature and sensitivity calibrations were done with indium, bismuth, zinc, aluminum, and gold standards supplied with the calorimeter for all heating rates (5, 10, and  $20^\circ\text{C}/\text{min}$ ). To correct the scanning rate dependence of the DSC data, the results for the temperature were obtained by extrapolating the onset temperatures to an isothermal situation by a linear regression method based on at least 5 runs. The reported error for the temperature resulted from the extrapolation. Heats of the first phase transition were calculated from the average of 5–6 runs. Gases evolved during thermal analysis were analyzed by a Bruker EQUINOX 55 FTIR spectrometer, which was directly coupled with the TG/DSC by a heated transfer line kept at  $150^\circ\text{C}$ . FTIR spectra of evolved gases were collected in a range of  $400$ – $4000 \text{ cm}^{-1}$  at a resolution of  $4 \text{ cm}^{-1}$ . A baseline correction was made before each run.

The thermochemistry of the self-assembly of silver alkanethiolates was studied in situ using an isoperibol CSC 4400 calorimeter. The synthesis conditions were mimicked in the calorimeter. About 25 mL of the thiol solution in acetonitrile was transferred to the reaction vessel in the calorimeter. After 30 min equilibration, a small dose (less than 1 mL) of silver nitrate solution also in acetonitrile was injected into the reaction vessel, and the heat of the reaction was measured. The heats were corrected to compensate for the dilution effects by extrapolating to the zero volume of the injected silver nitrate solution.

A Calvet-type twin microcalorimeter Setaram C80 was used to study the energetics of postsynthesis treatment of as-synthesized silver alkanethiolates. For these experiments, the mixture of toluene and silver alkanethiolate powder was loaded in a glass-lined stainless steel vessel at room temperature. The vessel was sealed to contain any volatile species. After the vessel was loaded into the calorimeter, it was allowed to equilibrate for 30 min at room temperature. The sample was then heated at a low ramp rate ( $0.1$ – $0.3^\circ\text{C}/\text{min}$ ) to a temperature of about  $110^\circ\text{C}$ . From the heating

(24) Bansebaa, F.; Ellis, T. H.; Kruus, E.; Voicu, R.; Zhou, Y. *Langmuir* **1998**, *14* (22), 6579.

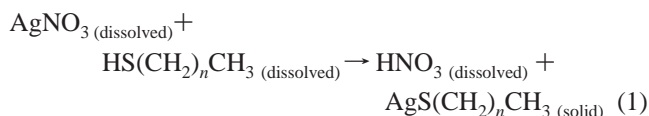
(25) Voicu, R.; Badia, A.; Morin, F.; Lennox, R. B.; Ellis, T. H. *Chem. Mater.* **2000**, *12* (9), 2646.

(26) Levchenko, A. A.; Moloy, E.; Parikh, A. N.; Navrotsky, A., manuscript in preparation.

scan, the heat of solution/melting in toluene was measured. Similarly, the heat of crystallization in toluene was deduced from the cooling scan.

## Results and Discussion

**Mechanism and energetics of formation of silver alkanethiolates.** The assembly of silver alkanethiolates is a multistep process that involves two major parts: the formation of an inorganic core associated with Ag and S coordination and stacking of bimolecular layers to form the three-dimensional structure. The first step occurs through direct interaction between silver and thiol group according to the following reaction:



From a thermodynamic viewpoint, the self-assembly of a thiol on metal surfaces is driven by the enthalpy factor  $\Delta H$  due to the highly stable metal sulfur chemical bond. Indeed, the entropy  $S$  decreases after adsorption and binding. This preset balance between negative  $\Delta H$  and negative  $T\Delta S$  motivated us to measure the formation enthalpy of silver alkanethiolate crystals. Previous electrochemical measurements yielded only the Gibbs free energy of the process. The formation of silver alkanethiolates from a reaction mixture occurs in a similar fashion: the negative  $\Delta S$  is compensated by a negative  $\Delta H$  as the thiolate crystals are formed.

A typical calorimetric response upon addition of the silver nitrate solution is depicted in Figure 2a. The reaction is highly exothermic, as expected. Only a single peak is observed. As seen from the changes in heat flow, the reaction for all alkanethiolates proceeds very quickly and is complete within a time interval of about 20 min. The actual reaction may occur even more quickly; the 20 min reaction time also reflects the response time of the calorimeter. The insert in Figure 2a shows the heat effect associated with the dilution of the thiol solution after injection of the pure acetonitrile into the reaction vessel. This heat effect is an order of magnitude smaller than the total enthalpy. Figure 2b represents the chain-length dependence of the formation enthalpy, which can be approximated by a straight line. Linear regression yields a chain-length independent component (intercept) of  $-137 \pm 6$  kJ/mol (the error comes from the extrapolation), which is related to the Ag–S bonding. This value is consistent with our ab initio calculations, which yielded 146 kJ/mol for the reaction enthalpy. The enthalpy becomes more exothermic as longer chains are confined within the inorganic framework. This stabilization results in a slope of  $-4 \pm 0.5$  kJ/mol per methyl group, associated with the energy released as methyl groups separated by solvent are brought together by the van der Waals forces and arranged in a three-dimensional structure. As the reaction proceeds, the precipitate of insoluble silver alkanethiolate crystals forms until all thiol is consumed.<sup>13,14,24</sup> The product  $\text{HNO}_3$  remains in solution.

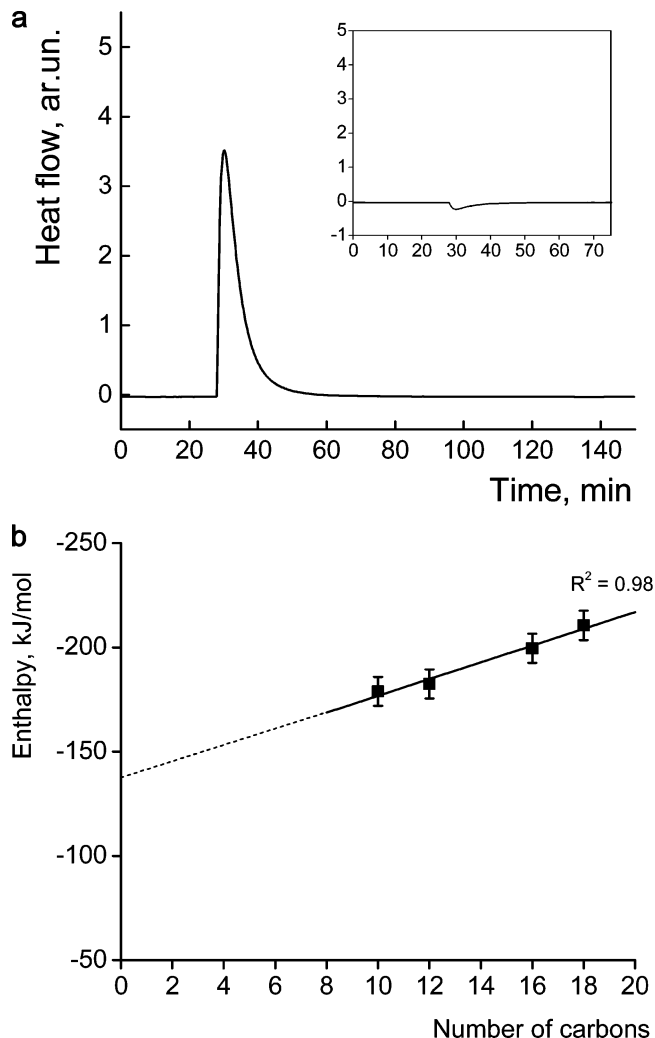


**Figure 2.** Typical in situ synthesis calorimetry scan for  $n = 9$  at room temperature (a). Enclosed is a calorimetric signal observed after injection of the pure solvent into a reaction vessel. Enthalpy deduced from in situ calorimetry results vs number of carbons ( $n + 1$ ) (b). The line is a fit to experimental data.

For comparison, one can consider a model reaction between silver nitrate and hydrogen sulfide to form silver sulfide and nitric acid



The reaction enthalpy from standard enthalpies of the reactants and products is  $-117$  kJ/mol,<sup>27</sup> which compares well with the enthalpy reported here, although the two reactions involve different structures. Another estimate of  $-160$  kJ/mol is also available for the S–Ag bond energy in the literature.<sup>28</sup>

It is impossible either to measure or to estimate the entropy contribution to the free energy of reaction 1 straightforwardly. Nevertheless, one should bear in mind that due to a loss of six degrees of freedom (three translational and three rotational) for each component when going from the solution to a precipitate, the entropy change should be significantly

(27) GTT-Technologies, T. C. a. *FactSage*, 5.3.

(28) Schlenoff, J. B.; Li, M.; Ly, H. *J. Am. Chem. Soc.* **1995**, *117* (50), 12528.

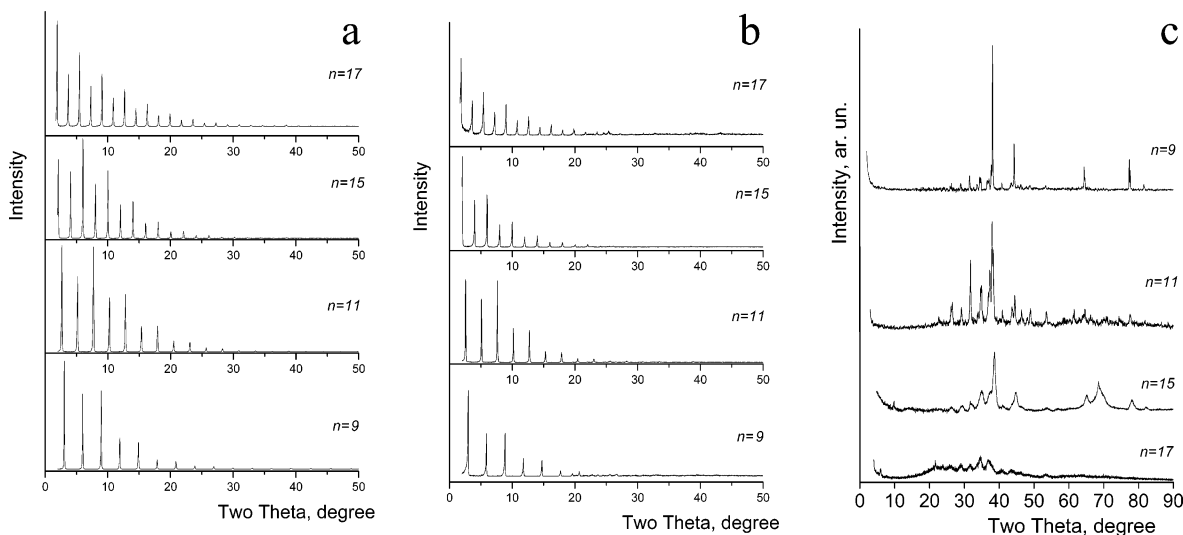


**Figure 3.** Powder X-ray diffraction data for selected long-chain silver alkanethiolates ( $\text{AgS}(\text{CH}_2)_n\text{CH}_3$ ,  $n = 9, 11, 15,$  and  $17$ ) recrystallized in toluene (a) and annealed at (b)  $155$  and (c)  $255$  °C for  $1$  h. The number of carbons is given in the figure.

negative. Indeed, Searle and Williams<sup>29</sup> estimated the entropy cost, associated with the transfer of a molecule from solvent into a solid, to be  $-45$  kJ/mol at room temperature in  $T\Delta S$  units, based on a correction to Trouton's rule<sup>30</sup> (similar entropies of condensation for a large number of liquids). Page and Jencks<sup>31</sup> postulated a similar entropy change of  $-50$  to  $-60$  kJ/mol associated with less translational and rotational degrees of freedom upon covalent bond formation.

Thus, the in situ synthesis calorimetry permitted us to capture the energetics that govern the alkanethiolate assembly with silver into the three-dimensional structure. Further analysis of the structure evolution and phase transitions in silver alkanethiolates gives deeper insight into the energetics and ordering of alkyl chains in a confined environment.

**Characterization of Recrystallized Silver Alkanethiolates by Powder X-ray Diffraction.** XRD analysis of as-synthesized samples was done previously by us<sup>13,14</sup> and others.<sup>11,12,15,24</sup> Here, the powder XRD patterns for the four silver alkanethiolates in Figure 3 conform to the previously proposed model<sup>11</sup> of a layered structure with an interlayer periodicity of approximately twice the chain length. Indeed, the patterns are dominated by a series of intense reflections, which can be straightforwardly assigned to the orders of diffraction from the layered bimolecular assemblies with large interlayer distances ( $b$ ) and  $0k0$  planes. Up to 20 reflections were detected. The observation of a high degree of translational order along the interlayer periodicity apparent from the patterns clearly establishes that the samples obtained by hot toluene recrystallization exhibit significantly improved purity with low structural defect contents.

The  $b$  parameters are given in Table 1. These values correspond to a tilt angle of  $14.5^\circ$  for alkyl chains in fully extended trans configurations. To estimate the correlation lengths or crystallite size of polycrystalline materials along this direction, the peaks were fitted using a pseudo-Voigt

**Table 1. Crystallographic Data for the Layered Structure and Mesophase**

$n$	Crystal	mesophase	
	$b$ (Å)	$d_{100}$ (Å)	$a$ (Å)
9	$29.92 \pm 0.02$	$23.4 \pm 0.2$	$27.0 \pm 0.3$
11	$34.80 \pm 0.03$	$25.5 \pm 0.3$	$29.4 \pm 0.3$
15	$44.43 \pm 0.01$	$28.1 \pm 0.3$	$32.4 \pm 0.3$
17	$49.22 \pm 0.03$	$29.6 \pm 0.4$	$34.1 \pm 0.4$

profile function to obtain half-widths. The corresponding crystallite size values derived from the half-widths using Scherrer's equation<sup>32</sup> are  $107 \pm 1$ ,  $76 \pm 1$ ,  $88 \pm 1$ , and  $81 \pm 2$  nm for  $n = 9, 11, 15,$  and  $17$ , respectively. These values are significantly higher than our previous estimates for unrecrystallized samples, further confirming that recrystallized samples offered significantly purer crystals with higher structural consistency.<sup>13</sup> A relatively wider range of estimated crystallite sizes may have resulted from the uncontrolled cooling rate under ambient conditions during recrystallization. From the interlayer distances of each compound, the number of AgSR bilayers is estimated to be 36, 23, 20, and 16 for  $n = 9, 11, 15,$  and  $17$ , respectively.

We also observed several other peaks in the XRD patterns, which are not orders of interlayer distance corresponding to the bimolecular layered structure. Their existence indicates registry in the packing of alkyl chains sandwiched between parallel inorganic sheets. These peaks are more pronounced for the samples heated above and then cooled below the first phase transition (Figure 3b). There is no agreement in the literature as to whether these reflections can be assigned unambiguously to the monoclinic unit cell and whether lattice constants can be calculated from them.<sup>15,33</sup> The low signal-to-noise ratios of these peaks, corresponding to the in-plane structure, precluded further analysis. Our detailed synchrotron XRD analysis and ab initio calculations confirm that the crystalline structure is characterized by the orthorhombic unit cell as the stable polymorph of

(29) Searle, M. S.; Williams, D. H. *J. Am. Chem. Soc.* **1992**, *114*, 4 (27), 10690.

(30) Everett, D. H. *J. Chem. Soc.* **1960**, 2566.

(31) Page, M. I.; Jencks, W. P. *Proc. Natl. Acad. Sci. U.S.A.* **1971**, *68*, 1678.

(32) Cullity, B. D. *Elements of X-ray Diffraction*; Addison-Wesley: Reading, MA, 1978.

(33) Bensebaa, F.; Ellis, T. H.; Kruus, E.; Voicu, R.; Zhou, Y. *Can. J. Chem.* **1998**, *76* (11), 1654.

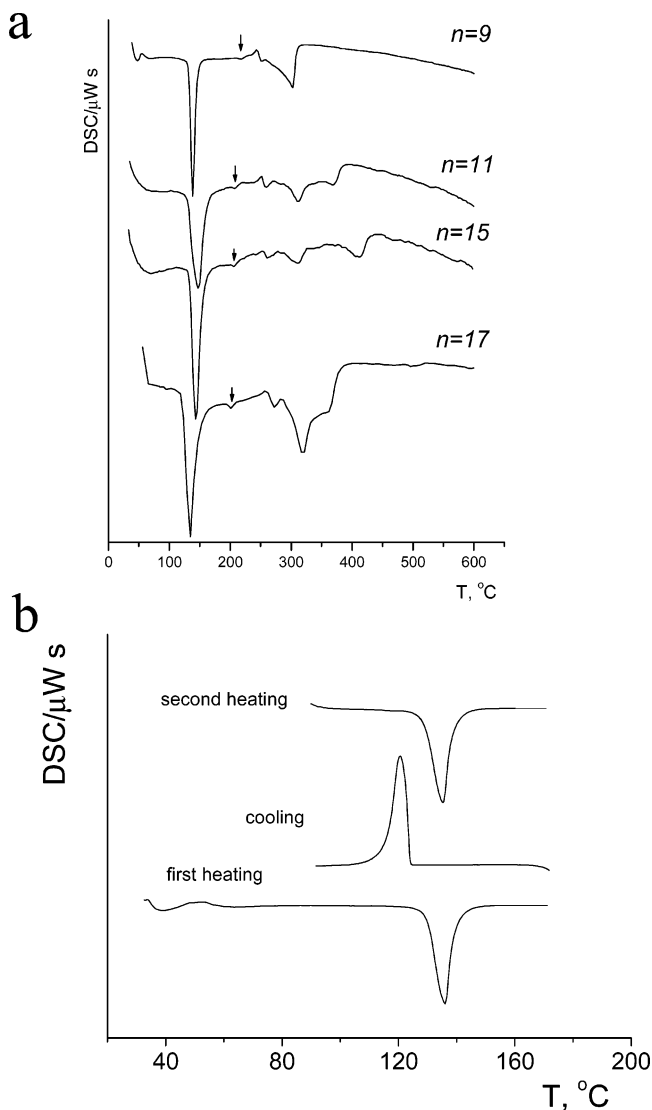


**Figure 4.** DSC data (a) for all the chain lengths at a heating rate of 5 °C/min (20 °C/min for  $n = 17$ ) and (b) multiple cycling DSC scans for  $n = 9$ .

silver alkanethiolates with alkyl chains tilted at 14.5° to the layers.

**DSC/TGA.** DSC data are shown in Figure 4a. The traces below 240 °C clearly reveal two endothermic transitions at approximately 130 and 210 °C for all four samples, clearly establishing chain-length independence of the transitions. The values are consistent with those reported previously by Baena and et al.<sup>12</sup> They attributed the low-temperature transition (130 °C) to the change from a crystalline phase to a micellar (columnar) mesophase and the higher temperature transition to the micellar to amorphous transition. In our experiments above 240 °C, the DSC signal became unstable and difficult to interpret (Figure 4a). Typical scans derived in multiple cooling and heating cycles, shown in Figure 4b, confirm the reversible thermodynamic character of the transition at 131 °C. As a result, the DSC traces lend themselves to a quantitative determination of the enthalpies and temperatures of the layered phase to mesophase transition. These values deduced from our DSC traces are tabulated in Table 2. The transition enthalpy clearly increases with the chain length of the alkyl substituents in the silverthiolates, whereas the transition temperature remains independent of the chain

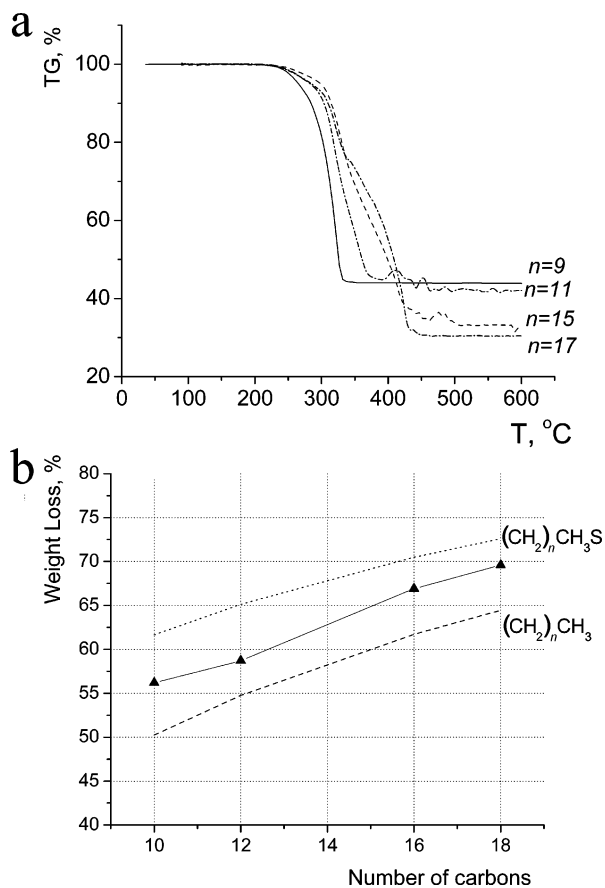


**Figure 5.** TGA data (a) and the final weight loss vs number of carbons (b).

**Table 2. Thermodynamic Characteristics of the Crystal-to-Mesophase Transition**

$n$	$T$ (°C)	$\Delta H$ (kJ/mol)	$\Delta S$ (J/K mol)
9	130.5 ± 0.5	35.3 ± 0.5	86.2 ± 1.0
11	131.1 ± 0.3	39.3 ± 2.7	97.2 ± 6.2
15	131.0 ± 0.5	53.7 ± 1.2	132.9 ± 3.8
17	131.1 ± 0.3	58.8 ± 2.2	145.5 ± 7.5

length (Table 2). The entropy of transition is also given; it varies with chain length to compensate for the variation in  $\Delta H$ .

Figure 5 also shows thermogravimetric analysis (TGA). The onset of material degradation is observed at ~220 °C for all silver alkanethiolates studied here, again independent of the chain length. No significant weight loss is observed above 350–370 °C for short chains ( $n = 9$  and 11) and above 430–440 °C for longer chains ( $n = 15$  and 17). The weight loss at the highest temperature compares well with the theoretical value calculated for the loss of a  $(\text{CH}_2)_n\text{CH}_3$  unit of the alkyl fragments. Our data indicate that the second transformation, which begins at ~220 °C, is accompanied by degradation of alkyl chain moieties, presumably leaving behind a Ag residue. The difference in theoretical and calculated weights of ~5% may arise from residual  $\text{Ag}_2\text{S}$  as discussed next.

**Evolved Gas FTIR.** Evolved gas FTIR provides a simple but powerful means to characterize the thermal degradation processes taking place above 200 °C and to identify their onset. FTIR spectra of evolved gases of all silver alkanethiolates heated above 210 °C show vibrational absorption

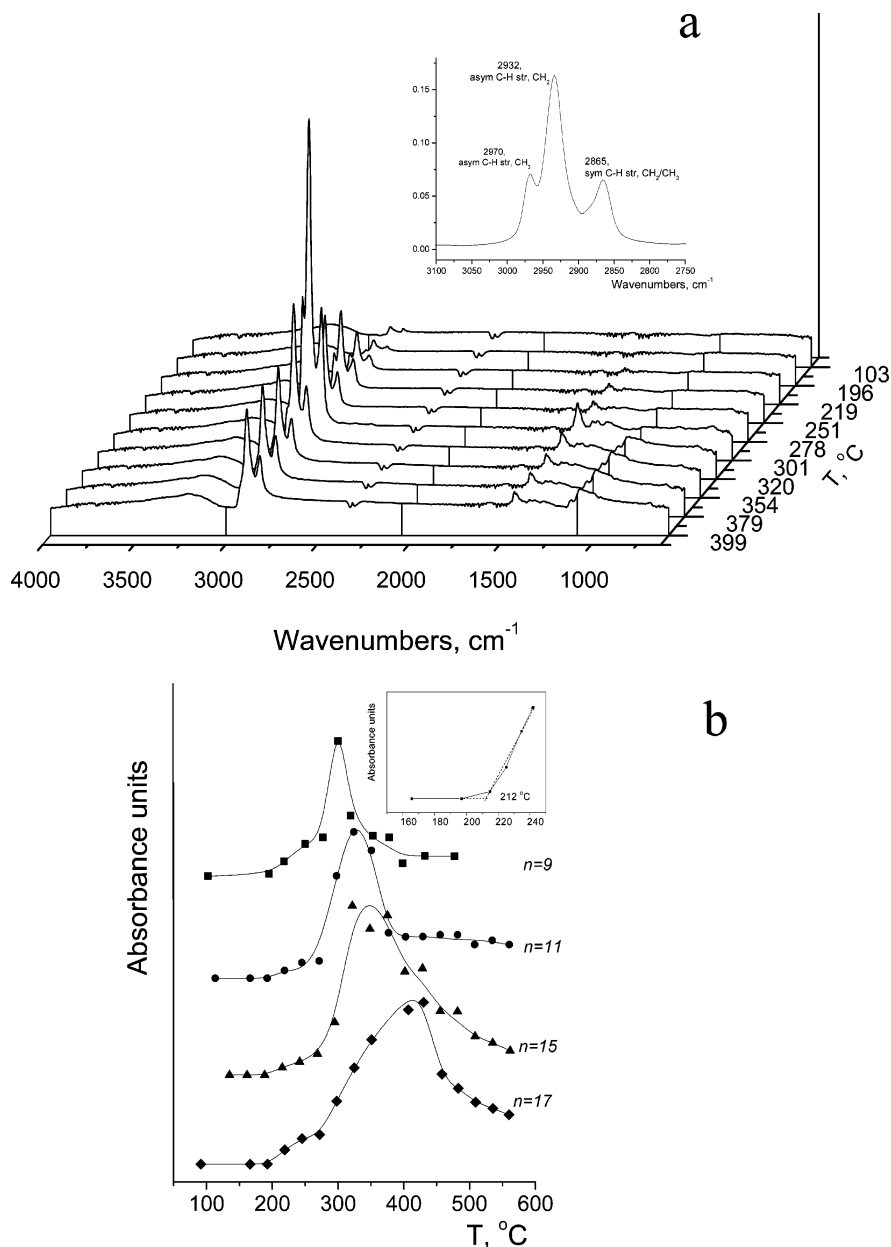


**Figure 6.** Evolved gas FTIR data. (a) Temperature evolution of FTIR spectra for one selected chain length ( $n = 9$ ). The evolved gas FTIR spectrum at 299 °C in the range of 3100–2750  $\text{cm}^{-1}$  for  $n = 9$  is shown in the upper right corner. (b) Temperature dependences of the integrated intensity due to the selected asymmetric methylene C–H stretching mode at 2932  $\text{cm}^{-1}$ . The temperature dependence of the integrated intensity for  $n = 17$  between 160 and 240 °C is shown in the upper right corner. The lines are guides for the eye.

bands that can be unambiguously assigned to the fragments of  $n$ -alkanes<sup>34–36</sup> (Figure 6a). Specifically, three strong bands are discernible at 2970, 2932, and 2865  $\text{cm}^{-1}$ . The band at 2865  $\text{cm}^{-1}$ , with a shoulder at 2885–2890  $\text{cm}^{-1}$ , is most probably a combination of two bands corresponding to symmetric C–H stretching of the  $\text{CH}_2$  ( $d^+$ ) and  $\text{CH}_3$  ( $r^+$ ) groups. The other two peaks can be assigned to asymmetric C–H stretching of the  $\text{CH}_3$  ( $r^-$ , 2970  $\text{cm}^{-1}$ ) and asymmetric C–H stretching vibration of the  $\text{CH}_2$  ( $d^-$ , 2932  $\text{cm}^{-1}$ ), respectively. Two bands at 1466 and 1380  $\text{cm}^{-1}$  can be assigned to C–H deformations of  $\text{CH}_2$  ( $\delta$ ) and  $\text{CH}_3$  ( $\alpha$ ),

respectively.<sup>37</sup> The higher frequency peaks for the evolved gas are considerably shifted with respect to those observed for long-chain substituents in solid silver alkanethiolates and long-chain alkanes in solid or liquid state but appear in the ranges typically observed for short-chain alkyl residues and gases.<sup>34–36</sup> Together with TGA, the evolved gas FTIR data signal the physical transformation, most likely via thermal degradation, of the organic phase in the silver alkanethiolate samples. Closer inspection of the temperature dependence of absorbance for the most intense band at 2932  $\text{cm}^{-1}$  permitted us to determine the onset temperature for the decomposition to be  $\sim 210$  °C. This inference is consistent with TGA data.

(34) Snyder, R. G.; Strauss, H. L.; Elliger, C. A. *J. Phys. Chem.* **1982**, 86 (26), 5145.

(35) Maroncelli, M.; Qi, S. P.; Strauss, H. L.; Snyder, R. G. *J. Am. Chem. Soc.* **1982**, 104 (23), 6237.

(36) Snyder, R. G.; Maroncelli, M.; Strauss, H. L.; Hallmark, V. M. *J. Phys. Chem.* **1986**, 90 (22), 5623.

(37) Bellamy, L. J. *The infrared spectra of complex molecules, Vol. 2: Advances in infrared group frequencies*; Chapman and Hall: London, 1980.

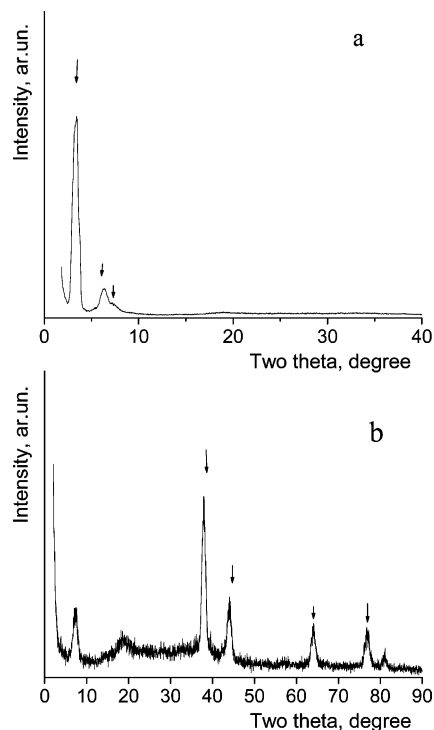


**Figure 7.** XRD patterns for the silver thiolate with  $n = 17$  for selected temperatures (a) 150–160 °C (arrows show hexagonal peaks) and (b) 220–230 °C (arrows show silver cubic peaks).

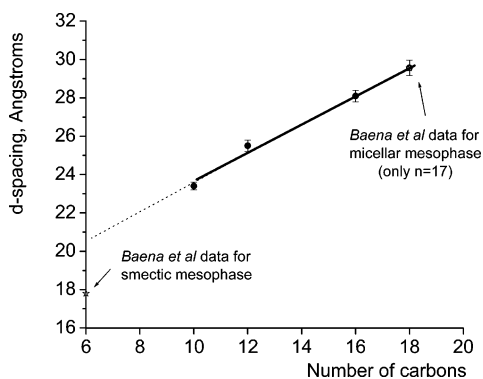


**Figure 8.** Dependence of the  $d$  spacing of the (100) peak of the hexagonal columnar mesophase on the number of carbons ( $n + 1$ ). The lines are fits to experimental data.

**XRD at Elevated Temperatures.** The XRD patterns at 150–160 °C (Figure 8) for all the chain lengths show two distinctive peaks at low angles below 10° ( $2\theta$ ). The first peak is a (100) reflection of the hexagonal lattice. The second peak is likely due to the overlap of (110) and (200) broad peaks. Positions of these reflections agree with the earlier proposed model of micellar structure (or columnar mesophase),<sup>12</sup> which is characterized by a 2-D hexagonal assembly of columns. These columns are formed by the correlated stacking of disks (rings) composed of eight R–S–Ag moieties as depicted in Figure 1b. Table 1 summarizes crystallographic characteristics for the mesophase. These data are in good agreement with those reported by Baena and co-workers<sup>12</sup> for one chain length ( $n = 17$ ). The correspondence in the structure of the mesophase for the four chain lengths tested here is confirmed by the linear increase of the hexagonal lattice parameter  $a$  with increasing chain length as seen in Figure 8.

The XRD patterns for temperatures above 210 °C show a single weak broad peak in the low angle region (Figure 7b). The peak cannot be assigned to mesophase reflections and must represent the formation of the degraded material. This is in good agreement with our previous observation that the FTIR peak position for the conformationally sensitive methylene stretching modes red-shift to 2855 and 2926  $\text{cm}^{-1}$ , comparable to values observed for disordered chains in the liquid and glass.<sup>37</sup> Several stronger X-ray peaks are also observed at high angles, corresponding to cubic silver.<sup>38</sup> For the samples obtained by long annealing for 1 h at 255 °C, other peaks, which do not belong to silver,<sup>38</sup> are also seen. They indicate the presence of the monoclinic modification of silver sulfide known as the low-temperature polymorph, argentite.<sup>39</sup>

**Phase Transition at 131 °C from Crystalline Phase to Mesophase.** When samples were heated to 155 °C, above the first transition temperature of 131 °C, and then cooled to room temperature, XRD patterns revealed the reversibility of the structural changes that attend the first transition. No noticeable change of the layered material structure, as deduced from the XRD patterns, occurred in many successive thermal cycles about the first transition temperature. Moreover, this complete reversibility was independent of the chain-length of the alkyl substituents as evident in the XRD patterns for all the sample types investigated here (Figure 3b).

The structure of the high-temperature phase is identified in this study as a columnar mesophase, thus supporting the model proposed by Baena et al.<sup>12</sup> Our MD simulations for the high-temperature phase are also in good agreement with the experimentally derived lattice parameters.<sup>26</sup>

Analysis of the DSC data suggests that the enthalpy of the phase transition increases linearly with the chain length yielding a slope of  $3.1 \pm 0.2$  kJ/mol per  $\text{CH}_2$  group (Figure 9a). In a previous study, Bensebaa et al.<sup>24</sup> reported that the temperature increases only slightly (about 5 °C) with the chain length for eight to 18 carbons. It is not clear from the data reported by Baena et al.<sup>12</sup> whether the first transition they measured was temperature-independent. Our data, derived using a structurally self-consistent set of recrystallized silver alkanethiolates, explicitly establish that, although the transition enthalpy varies, the temperature is invariant with chain length to  $\pm 0.6$  °C (Table 2) since at the thermodynamic transition temperature  $\Delta G = 0$ , implying that  $\Delta S = \Delta H/T$ , the entropy also varies with the chain length (see Figure 9b). The synergy between the chain-length dependent variations in  $\Delta H$  and  $\Delta S$  (enthalpy–entropy compensation) keeps the transition temperature constant across the sample series investigated.

Enthalpy–entropy compensation occurs in many chemical processes including complex dissociation, salvation, and ligand–receptor interactions.<sup>40</sup> This phenomenon is usually described as a linear relationship between enthalpy and

(38) Swanson, H. E.; Tatge, E. *Nat. Bureau Stand. Circ. (U. S.)* **1953**, *1*, 539.

(39) Frueh, A. J., Jr. *Z. Kristallogr., Kristallgeom., Kristallphys., Kristallchem.* **1958**, *110*, 136.

(40) Liu, L.; Yang, C.; Mu, T. W.; Guo, Q. X. *Chin. Chem. Lett.* **2001**, *12* (2), 167.



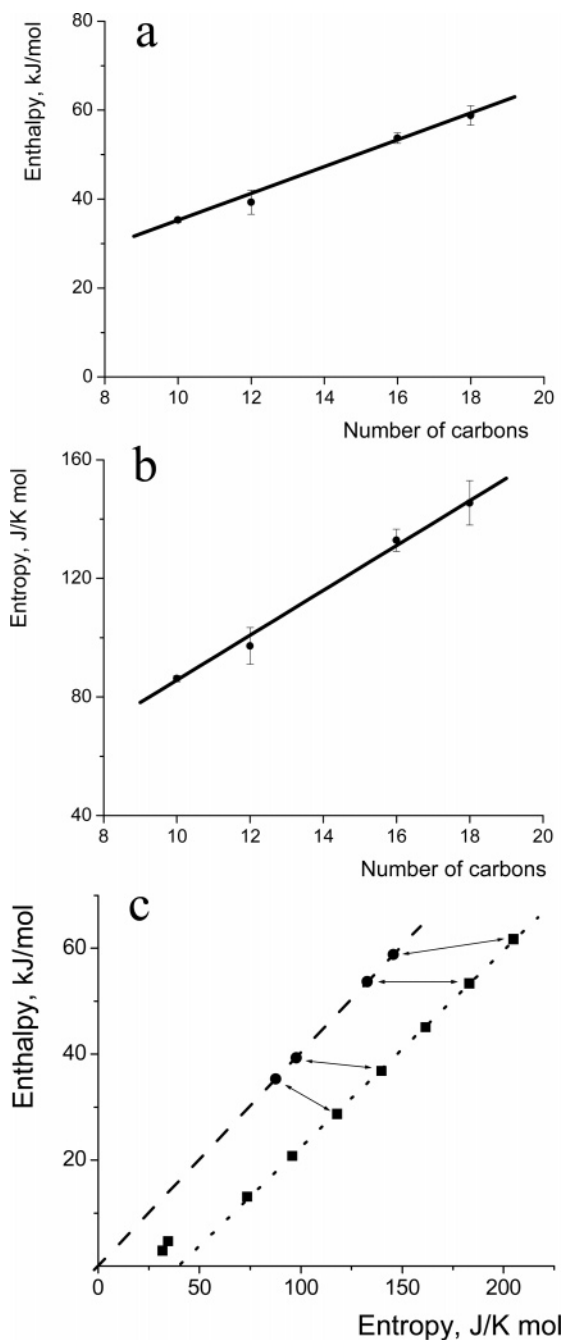


**Figure 9.** Enthalpy (a) and entropy (b) of the crystal-to-mesophase transition. The lines are fits to experimental data. Entropies are calculated from  $\Delta S = \Delta H/T$ . (c) Enthalpy vs entropy for the crystal-to-mesophase transition of silver alkanethiolates (circles) and melting of even  $n$ -alkanes with two to 18 carbons. The line, fitted through experimental data points for silver alkanethiolates, corresponds to a transition temperature of 131 °C. The line, plotted through experimental data points for  $n$ -alkanes, is a guide for the eye.

entropy, so the compensation effect, due to the simultaneous change of enthalpy and entropy, leads to a smaller net free energy dependence on structural and compensational parameters being varied. In silver alkanethiolates, the compensation effect is characterized by the linear relationship between enthalpy and entropy, which results in a quite rare phenomenon, namely, chain length independence of the transition temperature.

It is useful to recall that the enthalpy and temperature increase is linear with respect to the side-chain length at least

for 10–18 carbon atoms in side-chain polymers, such as in poly-L-glutamate<sup>41</sup> and poly( $n$ -acryl methacrylates),<sup>42</sup> and related to the side chain melting. In contrast, chain-length independent constant phase transition temperatures such as found here characterize another important class of organic–inorganic complexes obtained by intercalation, namely, metal alkylphosphonates,<sup>43</sup> where the constant transition temperature is attributed to the domination of electrostatic metal–phosphate interactions over the van der Waals forces between alkyl chains.

In this regard, we draw an analogy with  $n$ -alkanes. Williams et al. noted that a relatively large increase in entropy of melting for linear, branched, and cyclic alkanes, accompanied by a subsequent large increase in enthalpy, results in only a relatively small change in melting temperature (average 7 °C per methylene group for  $n$ -alkane chains with 10–18 carbons). They attributed this to the correlation between increased motion of alkyl chains in the melt (measured by  $\Delta S$ ) and decreased bonding (reflected in  $\Delta H$ ).

According to Wunderlich,<sup>44</sup> the melting entropy of  $n$ -alkanes contains three major contributions: positional, orientational, and conformational. However, the increase in entropy with chain length results predominantly from the conformational contribution alone, yielding values in a narrow range of 7–12 J/K mol per segment. In our analyses of silver alkanethiolates, the slope of the entropy of the main transition as a function of number of carbons is  $7.6 \pm 0.4$  J/K mol per carbon (Figure 9b). This value associated with the partial disordering of chains, which accompanies the crystalline–mesophase transition, is entirely consistent with the predictions from the Wunderlich model.<sup>44</sup>

Moreover, strong chemical bonding of alkyl chains to the silver framework in silver alkanethiolates leads to entropies 40–55 J/K mol lower than those in  $n$ -alkanes, although the enthalpies are generally comparable. Figure 9c shows an offset of the enthalpy–entropy dependence to lower entropy values. The line for silver alkanethiolates passes through zero, indicating constant temperature of the phase transition.

The intercept of the line for entropies in Figure 9b is  $10 \pm 5$  J/K mol, which may represent a contribution from the positional and orientation rearrangements of alkyl chains. This value is much lower than that for  $n$ -alkanes<sup>44</sup> and, therefore, further supports that, in contrast to alkane molecules, the alkyl chains of silver alkanethiolates are not allowed to slide past each other in the mesophase.

The analysis of the calorimetric data presented has shown that enthalpy–entropy compensation for silver alkanethiolates originates in a nontrivial manner because the enthalpy increase is comparable but the entropy increase is lower as compared to those of normal alkanes due to the tethering of the chains at the sulfur end (see Figure 9c).

(41) Watanabe, J.; Ono, H.; Uematsu, I.; Abe, A. *Macromolecules* **1985**, *18*, 8 (11), 2141.

(42) Hempel, E.; Huth, H.; Beiner, M. *Thermochim. Acta* **2003**, *403* (1), 105.

(43) Gao, W.; Dickinson, L.; Morin, F. G.; Reven, L. *Chem. Mater.* **1997**, *9* (12), 3113.

(44) Wunderlich, B. *Thermal analysis*; Academic Press: Boston, 1990.

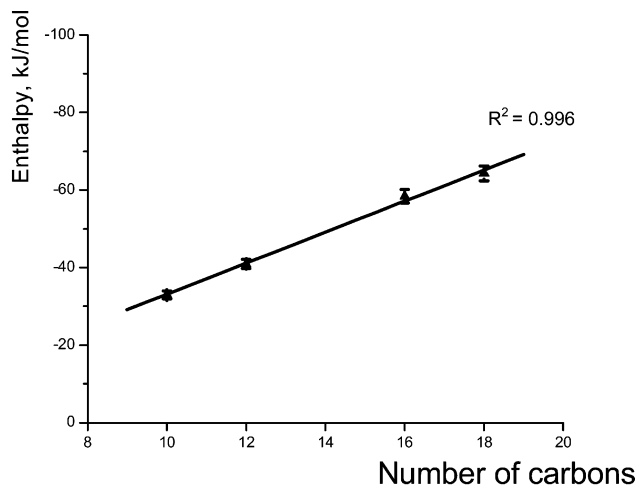


**Figure 10.** Enthalpy of dissolution vs number of carbons ( $n + 1$ ). The line is fit to experimental data.

In addition, we studied dissolution of the samples at elevated temperatures in toluene by in situ calorimetry using a Seteram C80 Calvet type microcalorimeter. We believed that this approach could mimic the assembly of the bimolecular sheets during the synthesis. The silver alkanethiolates are very insoluble in organic solvents. We found that a clear solution forms as the solid sample dissolves around 100 °C in toluene. The enthalpies of solution of the samples are 32.9, 41.0, 58.4, and 64.3 kJ/mol, respectively. Surprisingly, the enthalpies are comparable to that of the phase transition at 131 °C. As seen in Figure 10, they also demonstrate a linear dependence on chain length with a similar slope of  $4.0 \pm 0.4$  kJ/mol per methyl group. These results suggest that the chain melting triggers dissolution in toluene and that the dissolved material resembles the columnar mesophase discussed earlier. Moreover, the data suggest that energetically strong Ag–S bonds are intact in the dissolved state because their breakage must generate higher heat effects as established earlier by in situ synthesis calorimetry. Thus, a clear solution in toluene is not one of dissolved small molecules but probably consists of individual columns of the mesophase or other clusters (nanoparticles) derived from them.

**Chain Decomposition at ~210 °C.** In contrast to the first transition at 131 °C, the structural changes that attend the second chain-length independent transition at 210 °C are irreversible. When silver alkanethiolate samples were heated above the second transformation, subsequent cooling did not yield recognizable XRD patterns such as obtained for either the columnar mesophase or the low-temperature crystalline phase. In agreement with these observations, our previous FTIR spectroscopy data for silver *n*-dodecanethiolate<sup>14</sup> had suggested that the sample annealing beyond the second transition had led to an irreversible loss of spectral peaks due to the decomposition of the alkyl chain substituents. Our XRD data further extended these initial findings by revealing that the resulting structure strongly depended on the heating time. After prolonged annealing, all the samples regardless of alkyl chain lengths displayed at least some decomposition to the cubic silver phase and silver sulfide crystals evident in the appearance of silver and silver sulfide X-ray peaks (Figure 3c). Intermediate phases were also obtained with a shorter time (5–15 min) of annealing (not shown here). After

these elevated temperature annealing treatments, the visual appearance of the samples was no longer uniform and displayed pronounced color variations from the center to the edge of the powder aggregates. In light of a recent report<sup>45</sup> of the preparation of silver 5 nm nanoparticles from layered silver carboxylates by thermal decomposition, our observations of formation of mixed silver (and silver sulfide) crystallites with sizes larger than 10 nm suggest that the use of an analogous approach to make smaller nanoparticles from silver alkanethiolate precursors may be problematic.

Little is known about the mechanism of thermal decomposition and desorption of thiols.<sup>28,46,47</sup> For photooxidized SAMs on silver<sup>48</sup> and thermally decomposed SAMs on copper,<sup>8</sup> it has been reported that decomposition of thiol monolayers is accompanied not only by sulfur–metal bond breaking but also sulfur–carbon bond breaking. Our data also suggest that the desorption of thiols may occur at the silver interface due to scission of both Ag–S and S–C bonds to form silver, silver sulfide, and alkyl species. Although the complete picture of degradation is still unclear, we observe that approximately 50% of sulfur is evolved, leading to a mixture of Ag and Ag<sub>2</sub>S.

## Conclusions

The heat effects observed by in situ calorimetry conform to the mechanism of stepwise hierarchical assembly leading to the crystal growth. Similar to as-synthesized silver alkanethiolates, products of a recrystallization method proposed can be described by a self-consistent layered structure with an interlayer spacing of slightly less than twice the length of the alkyl chain. The orientational order, characterized by all-trans conformations of alkyl chains and a tilt angle of  $14.5 \pm 2^\circ$  to an inorganic core, is comparable to that for alkanethiolate monolayers on polycrystalline and Ag(111) surfaces. Two transitions observed at 131 and 210 °C are attributed to a reversible transition from the crystalline state to a mesophase, and subsequent irreversible decomposition, accompanied by formation of silver and silver sulfide crystals. The temperature of the first phase transition to the mesophase is independent of chain length. The enthalpy change, which varies with chain length, is compensated by the entropy change, which is mostly accounted for by conformational disordering of alkyl chains.

The thermochemical investigations of silver alkanethiolates presented in the paper not only reveal distinctive features of their formation mechanism and energetics but also have broader impact on future studies. The use of several complementary calorimetric techniques opens possibilities to study a broad class of self-assembled monolayers and hybrid organic–inorganic composites to give insights into bond formation and ordering, for example, coordination chemistry of sulfur atoms bonded to metal and organic counterparts.

(45) Lee, S. J.; Han, S. W.; Kim, K. *Chem. Commun.* **2002**, (5), 442.

(46) Han, S. W.; Lee, S. J.; Kim, K. *Langmuir* **2001**, *17* (22), 6981.

(47) Shibue, T.; Nakanishi, T.; Matsuda, T.; Asahi, T.; Osaka, T. *Langmuir* **2002**, *18* (5), 1528.

(48) Hutt, D. A.; Cooper, E.; Leggett, G. J. *J. Phys. Chem. B* **1998**, *102* (1), 174.

**Acknowledgment.** This research was supported by NSF Grant DMR 01-01391 to A.N. C.K.Y. and A.N.P. acknowledge support from the Office of Science, Department of Energy and Los Alamos National Laboratory. The authors thank Saliem

Than, a SEED student, for the synthesis of some silver alkane-thiolate samples and the SEED program for making it possible.

CM050961I